Cell, Vol. 114, 623–634, September 5, 2003, Copyright ©2003 by Cell Press

RraA: a Protein Inhibitor of RNase E Activity that Globally Modulates RNA Abundance in *E. coli*

Kangseok Lee,[1,7] Xiaoming Zhan,[3,4,7] Junjun Gao,[3] Ji Qiu,[3,4] Yanan Feng,[1] R. Meganathan,[6] Stanley N. Cohen,[1,2] and George Georgiou[3,4,5,*]

[1]Department of Genetics
[2]Department of Medicine
Stanford University School of Medicine
Stanford, California 94305
[3]Institute for Cell and Molecular Biology
[4]Department of Chemical Engineering
[5]Department of Biomedical Engineering
University of Texas at Austin
Austin, Texas 78712
[6]Department of Biological Sciences
Northern Illinois University
DeKalb, Illinois 60115

Summary

Ribonuclease E (RNase E) has a key role in mRNA degradation and the processing of catalytic and structural RNAs in *E. coli*. We report the discovery of an evolutionarily conserved 17.4 kDa protein, here named RraA (*r*egulator of *r*ibonuclease *a*ctivity A) that binds to RNase E and inhibits RNase E endonucleolytic cleavages without altering cleavage site specificity or interacting detectably with substrate RNAs. Overexpression of RraA circumvents the effects of an autoregulatory mechanism that normally maintains the RNase E cellular level within a narrow range, resulting in the genome-wide accumulation of RNase E-targeted transcripts. While not required for RraA action, the C-terminal RNase E region that serves as a scaffold for formation of a multiprotein degradosome complex modulates the inhibition of RNase E catalytic activity by RraA. Our results reveal a possible mechanism for the dynamic regulation of RNA decay and processing by inhibitory RNase binding proteins.

Introduction

The 118 kDa protein ribonuclease E (RNase E), which was discovered initially by its ability to generate p5S RNA from nascent ribosomal 9S RNA transcripts (Ghora and Apirion, 1978), is now known to have a central role in mRNA decay (for reviews, see Cohen and McDowall, 1997; Coburn and Mackie, 1999; Steege, 2000), the processing of tRNA (Li and Deutscher, 2002; Ow and Kushner, 2002), the pM1 RNA component of the ribozyme RNase P (Gurevitz et al., 1983), the tmRNA-mediated control of mRNA quality (Lin-Chao et al., 1999), and the regulation of DNA synthesis by ColE1-type plasmids (Lin-Chao and Cohen, 1991). Homologs of RNase E or of its close relative, RNase G, have been identified in, or inferred to exist from, DNA sequence analysis of more than 50 bacterial species, as well as Archae and plants (Lee and Cohen, 2003). The cleavage of substrates by RNase E occurs in A+U rich segments of single strand regions, although there is no simple relationship between substrate sequence and the phosphodiester bond cleaved (Cormack and Mackie, 1992; Mackie, 1992; Lin-Chao et al., 1994, McDowall et al., 1994, 1995). Whereas the extent of 5′ phosphorylation of substrates profoundly influences the cleavage rate and substrate binding by RNase E (Mackie, 1998, Feng et al., 2002), the enzyme attacks substrates processively or quasi-processively in the 3′ to 5′ direction (Feng et al., 2002) and can remove poly(A) tails from RNA molecules (Huang et al., 1998; Walsh et al., 2001). In vivo, RNase E production is autoregulated by cleavage of its own transcript (Mudd and Higgins, 1993; Jain and Belasco, 1995).

RNase E contains three functionally distinct domains: the N-terminal region, which is responsible for the preferential partitioning of the protein near the cell membrane (Liou et al., 2001) and contains the enzyme's catalytic domain (McDowall and Cohen, 1996), an arginine-rich central region which has strong RNA binding ability (Taraseviciene et al., 1995; McDowall and Cohen, 1996), and a C-terminal half (CTH) that provides a scaffold for the interaction of multiple proteins. The interacting proteins, which together with RNase E, form a complex termed the "degradosome" (Carpousis et al., 1994; Py et al., 1996; Miczak et al., 1996; Vanzo et al., 1998; Liou et al., 2001, Leroy et al., 2002), include the 3′ exonuclease polynucleotide phosphorylase (PNPase) (Carpousis et al., 1994) and a helicase capable of augmenting PNPase activity (Py et al., 1996; Miczak et al., 1996). However, whether degradosome formation enhances the rate of cleavage by RNase E is controversial (Lopez et al., 1999; Ow and Kushner, 2000). RNase E additionally has been shown to be capable of interacting with poly (A) polymerase (Raynal and Carpousis, 1999), and ribosomal protein S1 (Kalapos et al., 1997; Feng et al., 2001).

The processing of RNAs by RNase E is known to be affected by anaerobiosis during *E. coli* cell growth (Georgellis et al., 1993) and also to occur prominently in transcripts that encode proteins involved in energy-generating pathways (Lee et al., 2002; Bernstein et al., 2002). While these findings suggest that RNase E activity may be affected by cell physiology, little is known about cellular mechanisms that may modulate the degradation of RNA by RNase E. During experiments aimed at identifying genes whose overexpression enhances disulfide isomerase activity in *E. coli*, we identified a *trans*-active *r*egulator of *R*Nase E *a*ctivity, which we here name RraA. We show that RraA which, like RNase E, is widely distributed among bacteria and plants and increases disulfide isomerase production in *E. coli* by increasing the stability of mRNA encoding the disulfide isomerase, DsbC. We further show that RraA interacts with RNase E to inhibit its endoribonuclease action, that binding of RraA to RNase E and downregulation of RNase E activity are

*Correspondence: georgiou@che.utexas.edu
[7]These authors contributed equally to this work and are listed alphabetically.

modulated by the CTH, and that the effects of RraA on RNase E lead to global changes in RNA abundance, as well as to functionally altered gene expression. RraA thus represents a prototypical *trans*-acting modulator of RNase E activity and consequently of RNA turnover.

Results

Identification and Isolation of *rraA* in a Functional Screen for Genes that Enhance Disulfide Bond Isomerization in the *E. coli* Periplasm

In bacteria, the oxidation of protein thiols in secreted proteins is mediated by the soluble enzyme DsbA. The rearrangement of nonnative protein disulfide bonds is mediated by the disulfide isomerase DsbC, which is essential for the folding of eukaryotic proteins with multiple disulfide bonds expressed in the bacterial periplasmic space and to a lesser extent, by its homolog DsbG (Kadokura et al., 2003) Notably, human tissue plasminogen activator (h-tPA), a protease that converts plasminogen to plasmin and contains a total of 17 disulfide bonds, is expressed in a catalytically active form in *E. coli* only in cells that produce elevated levels of DsbC (Qiu et al., 1998).

Using a plate assay that detects colonies showing enhanced folding of h-tPA (see Experimental Procedures), we sought to identify genes whose IPTG-induced overexpression from a multicopy plasmid resulted in increased disulfide bond isomerization activity. A genomic DNA fragment from a bacterial clone that gave a large clearance zone on fibrin plates was studied further, and the single open reading frame (ORF) encoded within that fragment was subcloned downstream from a trc promoter in pTrc99A. To better quantify the effect of this ORF on the folding yield of multidisulfide proteins, we employed v-tPA, a truncated variant of h-tPA (Bessette et al., 2001). Whereas cells expressing h-tpA alone give no clearance of fibrin plates, colonies expressing v-tPA give a weak halo thus providing a more meaningful baseline. Lysate from cells coexpressing the isolated ORF and v-tPA gave a full clearance zone with four times larger diameter relative to cells expressing v-tPA alone (Figure 1A).

Western blot analysis revealed that the expression of this gene product resulted in a 5-fold increase in the steady-state level of DsbC protein but did not affect the amount of other periplasmic proteins, such as DsbA (Figure 1B). This increase was observed in different genetic backgrounds, in minimal or rich media, and in cells grown under either aerobic or anaerobic growth conditions.

To determine whether the observed increase in DsbC protein level had resulted from an increase in *dsbC* transcription, we constructed a chromosomally encoded fusion in which the promoter region of *dsbC* gene was placed upstream from a promoterless *lacZ* gene. Whereas no increase in β-galactosidase activity was detected following IPTG-induced expression of the cloned gene, suggesting that the transcription of *dsbC* was not affected (data not shown), RNase protection assays revealed a more than 5-fold increase in the half-life of the *dsbC* transcript (0.8 min to >4 min). The steady-state abundance of *dsbC* mRNA was also increased under

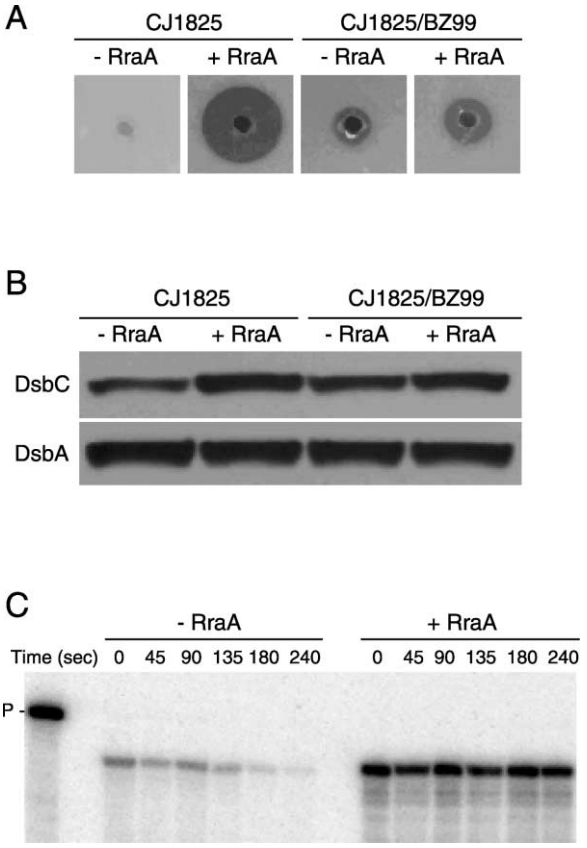

Figure 1. RraA Increase Disulfide Bond Isomerization by Affecting the Stability of the *dsbC* Transcript

(A) tPA fibrinolytic activity in cell lysates coexpressing v-tPA and RraA. Cells were grown to midexponential phase in rich media at 37°C, harvested and lysed in a French press, and 15 μg of total cell lysate protein was spotted on fibrin plates. Clearance zones after 24 hr are shown.

(B) Western blot of DsbC and DsbA levels in cells grown and harvested as in (A). Equal amount of total cell protein was loaded in each lane.

(C) DsbC mRNA decay. Cells were grown to midexponential phase and induced with 0.5 mM IPTG. 1.5 hr after induction rifampicin was added to a final concentration of 200 μg/ml. Samples were collected at different time points and RNA was extracted and quantified spectrophotometrically. 10 μg of total RNA was used for RNase protection assay. P, free probe-containing sequence complementary to the first 250 bp of *dsbC*.

these conditions (Figure 1C, t = 0 time point). Collectively, these findings suggested that the enhanced disulfide isomerization activity in the bacterial periplasm resulted from the stabilization of *dsbC* transcripts and a consequent increase in the steady-state level of DsbC protein.

DNA sequence analysis of the *E. coli* gene whose overexpression stabilized *dsbC* mRNA showed that it was identical to an open reading frame annotated in the NCBI database as *menG*. This open reading frame is located at 88.7 min in the *E. coli* chromosome and encodes a 17.4 kDa protein. *menG* had been assigned in the database entirely on the basis of sequence analysis that had suggested it encodes an enzyme with S-adenosyl-L-methione-dependent methyltransferase activity

capable of catalyzing the methylation of demethylmenaquinone, the last step in the biosynthesis of the electron transport mediator menaquinone (Meganathan, 1996). However, our examination of the biochemical function of the gene indicated that it does not in fact catalyze the methylation of demethylmenaquinone: neither multicopy expression of *menG* nor deletion of the entire gene (in strain JQ004) had any effect on the ratio of quinone:menaquinone:demethylmenaquinone in cells grown under aerobic or anaerobic conditions and further, the purified protein product of this gene failed to methylate demethylmenaquinone in the presence of S-adenosyl L-methionine (data not shown). Additionally, the crystal structure of the product of *menG* revealed no evidence of a S-adenosyl L-methionine binding site (A.F. Monzingo et al., submitted). We therefore concluded that the assignment of *menG* in the database is incorrect, and on the basis of experiments described in this report have designated the gene instead as *rraA* (*r*egulator of *r*ibonuclease *a*ctivity *A*).

RraA Interacts with RNase E In Vivo

A separate search for chromosomal lesions that enhance disulfide bond isomerization had resulted in the isolation of eight mutants that confer increased synthesis of DsbC protein by stabilizing its transcript (Zhan, 2002; X.Z., J.G., C. Jain, M. Cieslewicz, J.R. Swartz, and G.G., unpublished data); five of the eight mutants were found to be allelic to *rne*, which encodes RNase E, and an additional two mutants resulted in a significant reduction in RNase E activity in trans. The observed similarity between the phenotypes of the chromosomal *rne* mutants and those conferred by multicopy expression of *rraA* led us to speculate that the latter might also exert its effect through modulating RNA processing by RNase E.

RNase E autoregulates its own expression in cis, largely by cleaving its mRNA within the 5′ UTR (Mudd and Higgins, 1993; Jain and Belasco, 1995); consequently, production of RNase E is inversely affected by changes in the catalytic activity of the enzyme (Jain and Belasco, 1995). Consistent with the notion that RraA overexpression may decrease the activity of RNase E, Western blot analysis revealed that the steady-state level of RNase E is increased upon induction of RraA synthesis (data not shown). Similarly, analysis of β-galactosidase activity expressed from a chromosomal *rne-lacZ* fusion in which the 5′-UTR of the *rne* gene and the coding sequence for the N-terminal 181 amino acids of RNase E protein were fused upstream to *lacZ* in *E. coli* strain CJ1825 (Jain and Belasco, 1995), showed a 3- to 4-fold increase in β-galactosidase activity following induction of RraA synthesis (Figure 2A). Notably, the observed increase in the β-galactosidase activity from the *rne-lacZ* fusion in strain CJ1825 is comparable to that obtained by Jain et al. (2002) under conditions where RNase E is expressed at approximately 10%–15% of its normal level. The level of β-galactosidase activity from CJ1825/BZ99, which contains a truncated version of the *rne* gene encoding a protein consisting of only the catalytic, N-terminal domain (amino acid 1 to 602) of RNase E (Kido et al., 1996) and includes *rne-lacZ* fusion, was increased by 30% following induction of RraA synthesis (Figure 2A).

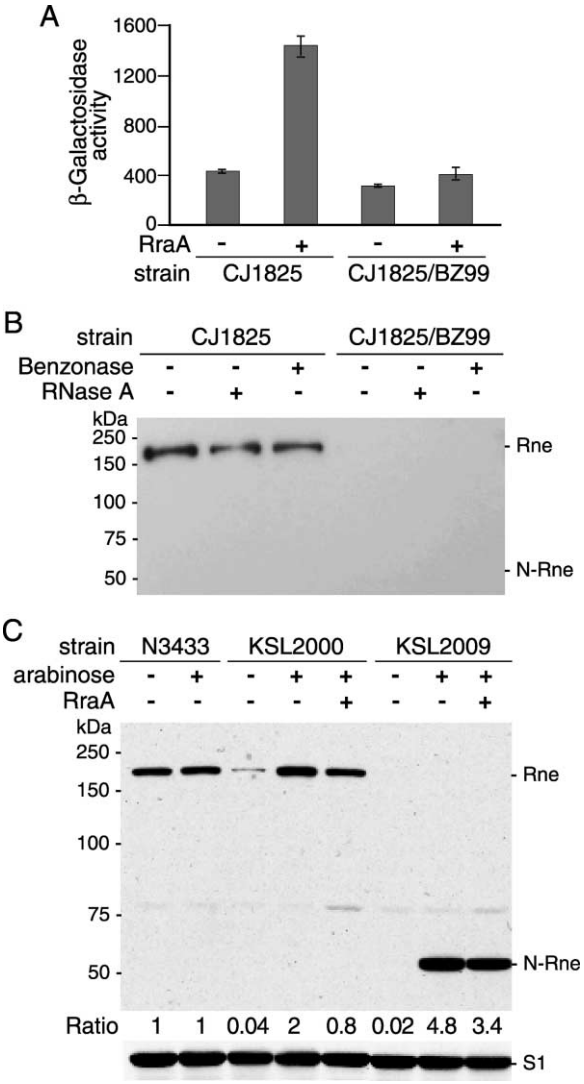

Figure 2. Interaction of RraA and RNase E In Vivo

(A) β-galactosidase activity (in Miller units) expressed from a chromosomal *rneE:lacZ* fusion. Cells transformed with pTrc99A and pTrc99A-RraA were grown in rich media and the synthesis of RraA was induced at an A_{600} ~0.2. 1.5 hr after induction the cells were assayed for β-galactosidase activity.

(B) Coprecipitation of RNase E with biotinylated RraA. Proteins coprecipitated using streptavidin-conjugated agarose beads were analyzed by Western blot using anti-RNase E polyclonal antibody (kindly provided by Dr. Kushner) as indicated in the Experimental Procedures.

(C) Western blot analysis of RNase E abundance in the absence of autoregulation in *E. coli* KSL2000 and KSL2009. The membrane was probed with anti-RNase E monoclonal antibody (upper image), stripped as indicated in Experimental Procedures and reprobed with anti-S1 polyclonal antibody (Feng et al., 2001) to provide an internal standard to evaluate the amount of cell extract in different lanes. Ratios were calculated by setting the signal of RNase E band in N3433 as 1 and normalized using signals from the S1 bands.

To elucidate the basis for the observed decrease in RNase E activity in vivo by RraA overexpression, we examined the interaction between RraA and RNase E by coprecipitation experiments. Briefly, an in vivo biotinylated version of RraA was constructed by fusing a 21

amino acid C-terminal extension (Biotag) encoding a peptide substrate of the *E. coli* biotin holoenzyme synthetase (BirA) (Schatz, 1993). As the RraA crystal structure indicates that the C-terminal is surface-exposed (A.F. Monzingo et al., submitted), we expected that addition of the C-terminal extension would not disrupt the tertiary structure of the protein; indeed, expression of the RraA-Biotag protein conferred the same phenotypes as unmodified RraA including increased DsbC accumulation and a 4-fold higher β-galactosidase activity expressed from the chromosomal *rne-lacZ* fusion (data not shown). Following precipitation using streptavidin-conjugated beads, Western blot analysis revealed the presence of RNase E in the precipitate fraction from cells expressing RraA-Biotag, but not in precipitates from control cells expressing scFv (single chain antibody variable region fragment)-Biotag or DsbA-Biotag fusion proteins or from cells transformed with empty vector. Importantly, the coprecipitation of RNase E by RraA-Biotag was not affected by treatment with RNase A or Benzonase nuclease, suggesting that nucleic acids do not represent a critical component of the complex between the two proteins (Figure 2B).

Further investigation revealed that the binding of RraA to RNase E lowers the steady-state level of the enzyme in vivo, presumably by affecting its stability to proteolytic degradation. In these experiments, autoregulation of RNase E was circumvented by using a strain in which the chromosomal *rne* gene had been inactivated and instead RNase E was expressed from an *rne* gene lacking the 5′ UTR and placed downstream from the arabinose-inducible P_{BAD} promoter in plasmid pSC101. In the resulting strain, KSL2000 (Lee et al., 2002), the synthesis of RNase E is controlled solely by the concentration of arabinose. The amount of RNase E protein in KSL2000 with or without *rraA* coexpression was determined by Western blotting using the ribosomal protein S1 as an internal standard (Figure 2C). The full-length RNase E to S1 ratio was reduced reproducibly by 60% and the ratio of RNase E catalytic domain (amino acids 1–498) to S1 in KSL2009 by 30% upon expression of RraA, indicating that the presence of RraA results in reduction of the steady-state level of RNase E polypeptide. The molar ratio of RraA monomer to RNase E in KSL2000 was estimated by Western blot band intensity to be 70 when RraA was overexpressed, whereas it was 20 in KSL2009 during overexpression (data not shown).

RraA Binds to RNase E and Inhibits Its Catalytic Activity In Vitro

Surface plasmon resonance analysis on a BIACORE 3000 instrument was employed to quantitatively analyze the interaction between RNase E and RraA. Full-length His-tagged RNase E and bovine serum albumin (BSA) were coupled on different flow cells of a CM5 chip under conditions that give low resonance units, as required to prevent rebinding effects. RraA was injected as analyte at different concentrations and its binding to the ligand was determined by the difference in response unit (RU) change upon injection between RNase E-coupled flow cell and the BSA-coupled flow cell. An equilibrium dissociation constant (K_D) of 26 μM was calculated from the data presented in Figure 3A by steady-state analysis.

Gel shift assays revealed no evidence for the binding of RraA to RNA, and excess RraA or BSA failed to inhibit the binding of RNA to RNase E. In contrast, addition of total RNA from *E. coli* abolished the binding of RNA to RNase E under the same conditions (Figure 3B). Furthermore, gel shift assays revealed that RraA does not affect the binding of pM1 to RNase E, supporting the view that inhibition of decay is mediated by a reduction of the ability of the enzyme to carry out hydrolysis of phosphodiester bonds rather than by an effect of RraA on substrate binding by RNase E. This result and the fact that coprecipitation of RNase E by RraA was not affected by the addition of nucleases (Figure 2B) support the notion that RNA is neither bound directly by RraA nor is part of the RNase E:RraA complex.

M1, the 377 nt catalytic component of the t-RNA processing ribozyme RNase P, is generated by the processing of a 415 nt precursor RNA (pM1), which is cleaved at sites near the 3′ end by RNase E. RraA inhibited the processing of pM1 in vitro (Figures 3C and 3D). 50% inhibition was observed at a 10:1 molar ratio of RraA monomer to purified full-length RNase E and the concentration of RraA was 0.5 μM under the assay conditions used. The concentration of RraA that causes 50% inhibition of RNase E-mediated RNA cleavage (Ki) varied depending on RNA substrate; the Ki for cleaving the 13 base oligonucleotide BR13 (McDowall et al., 1995) was 2.5 μM (data not shown). As gel filtration analysis (Figure 3E) and also the crystal structure of RraA solved at 2.0 Å (A.F. Monzingo et al., submitted) reveal that the protein is a trimer, we concluded that approximately a 3:1 molar excess of RraA trimer over RNase E monomer is required for inhibition. Under the conditions used in this assay and using GGG-RNAI as a substrate (Helmer-Citterich et al., 1988), RraA, even at 100-fold excess, had no effect on the catalytic activity of *E. coli* RNase G (data not shown), an RNase E-related protein whose overexpression was shown to complement deletion mutants in RNase E (Lee et al., 2002).

The Presence of the CTH Region Is Required for High-Affinity Binding of RNase E to RraA

The C-terminal half of RNase E serves as a scaffold for the binding of the major degradosome components RhlB, PNPase, and Enolase (Py et al., 1996, Miczak et al., 1996). In *E. coli* strain CJ1825/BZ99, the yield of folded, catalytically active tissue plasminogen activator (Figure 1A, samples 1 and 3) and the accumulation of DsbC protein were both increased, compared to the isogenic parent CJ1825. Expression of RraA in CJ1825/BZ99 increased the size of the fibrin clearance zone relative to cells transformed with empty plasmid. However, the RraA-mediated increase in tPA activity observed in *E. coli* CJ1825/BZ99 was noticeably lower than in CJ1825 cells that express the full-length RNase E. Additionally, in CJ1825/BZ99, RraA exerted only a slight, albeit reproducible, effect on the autocatalytic processing of the *rne* gene 5′ UTR, as determined by the level of β-galactosidase activity expressed from the *rne-lacZ* fusion (Figure 2A). Furthermore, the results of similar coimmunoprecipitation experiments described in Figure 2B using *E. coli* strains expressing RNase E having deletions in the CTH domain (Leroy et al., 2002) showed that all of these mutant RNase E proteins were able to interact with RraA regardless of the position of the deletion in the CTH (data not shown).

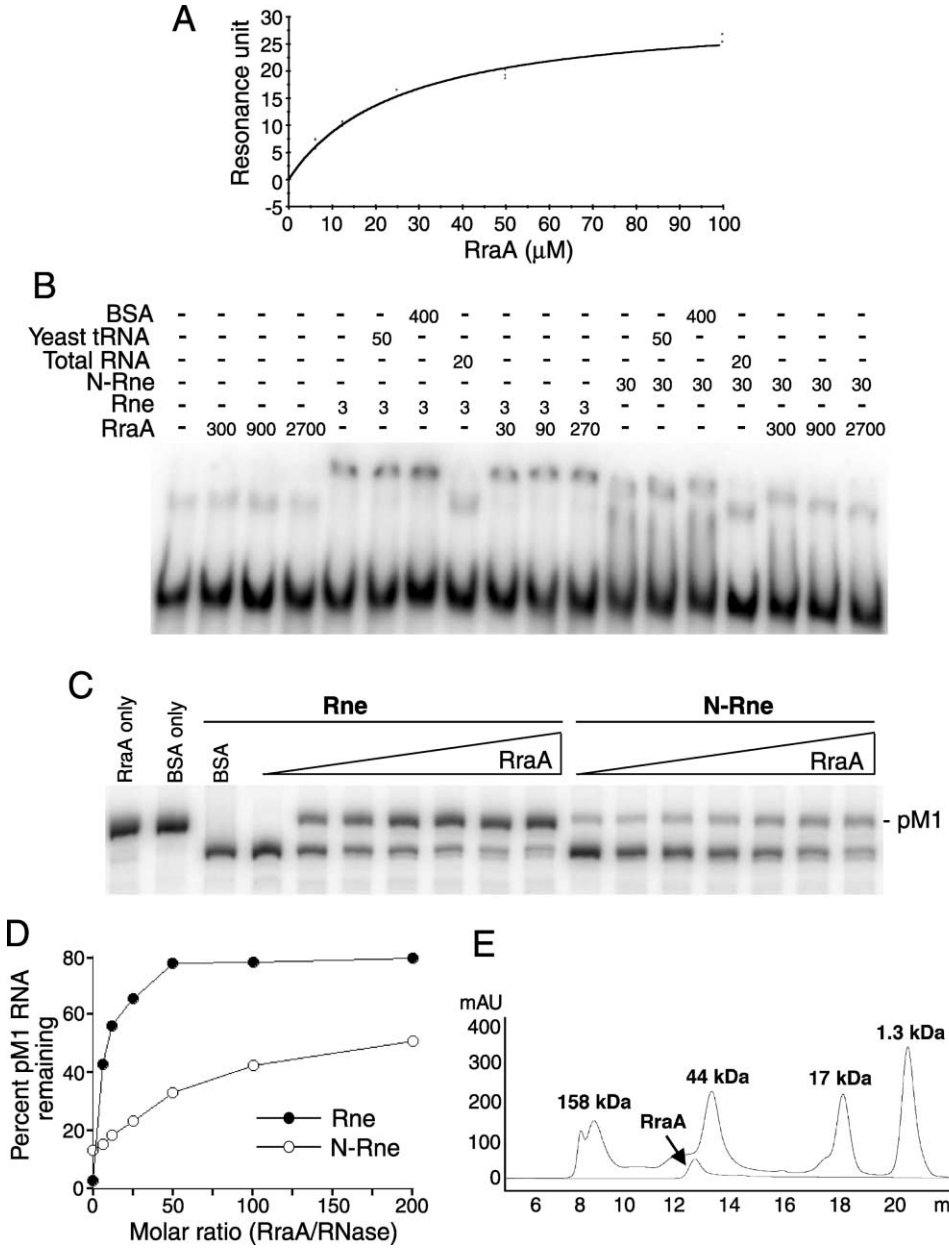

Figure 3. Interaction of RraA with RNase E In Vitro

(A) Steady-state analysis of surface plasmon resonance data. The resonance units obtained from sensorgrams were plotted against concentration of RraA and fitted with a steady-state model. The experimental R_{max} was 31.2 RU and Chi^2 was 1.14.

(B) Effects of RraA on RNA binding activity of RNase E. 50 ng of internally labeled pM1 RNA were incubated at room temperature for 10 min with proteins that were preincubated on ice for 10 min. Yeast tRNA and total *E. coli* RNA were used as nonspecific and specific competitors, respectively, for pM1 RNA. Numbers indicate molar ratios to pM1 RNA in reaction mixtures except for the total RNA (ratio of absolute amount).

(C) RraA inhibition of pM1 processing by RNase E in vitro. Two picomoles of internally labeled pM1 RNA were incubated with 100 ng of RNase E, or 200 ng of N-RNase E with varying concentrations of RraA, 8 μg of RraA, or 8 μg of BSA in 20 μl of 1× cleavage buffer at 37°C for 30 min for RNase E, or for 90 min for N-RNase E, RraA only, or BSA only controls.

(D) The percentage of uncleaved pM1 in the gel shown in C was quantitated using a Molecular Dynamics Phosphoimager and plotted as a function of the molar ratio of RraA/RNase E in the assay.

(E) Gel filtration analysis. Purified RraA and gel filtration protein standards were run on a FPLC Superdex 200 column (Amersham Biosciences) and the protein concentration (determined by the absorbance at 280 nm and reported as mAU) was monitored as a function of elution volume. Top line: Gel filtration protein standards. Bottom line: Purified RraA.

In vitro, RraA also inhibited the cleavage of pM1 by the N-terminal catalytic domain of RNase E. However the inhibitory effect of RraA was weak and the maximum inhibition of pM1 processing was 45% at the highest concentration of RraA used (200-fold molar excess of monomer over N-terminal catalytic domain protein). By comparison, with the full-length RNase E protein, saturating concentrations of RraA (50-fold molar excess of monomer over RNase E) gave 80% inhibition. Further, the IC_{50} value for the inhibition of the N-terminal catalytic

domain by RraA was at least 16-fold higher compared to the value measured with full-length protein. In control experiments, BSA even at a 200-fold molar excess had no effect on the processing of pM1 either by the full-length RNase E or by the N-terminal catalytic domain.

Efforts to detect a complex between the biotinylated RraA and the N-terminal region of RNase E in vivo by coprecipitation (Figure 2B) or by Far Western blot (data not shown) were unsuccessful. Similarly, an interaction between the respective purified proteins in vitro was not detected by surface plasmon resonance at RraA concentrations up to 200 μM. Measurements at higher concentrations could not be performed because RraA formed soluble higher molecular weight aggregates under these conditions.

RraA Globally Regulates the Half-Life and Abundance of *E. coli* Transcripts

We wished to examine the inhibitory effect of RraA on the stability of RNase E substrates in the absence of possible compensatory effects resulting from the autoregulation of the level of the enzyme in the cell. This was accomplished using *E. coli* strains KSL2000 and KSL2009, in which the synthesis of RNase E and the N-terminal catalytic domain respectively, is under the control of the arabinose promoter and which produce *rne* transcripts lacking the 5′ UTR site that is subject to attack by RNase E. Cells transformed with pTrc-RraA were grown in the presence of arabinose and expression of RraA was induced by addition of 0.5 mM IPTG. RraA expression in KSL2000 resulted in a 10-fold increase in the amount of intact pM1 transcript (Figure 4A). While expression of RraA also caused a 2.5-fold reduction in the steady-state level of RNase E protein (Figure 2C), it does not appear that the pM1 stabilization is due solely to the lower amount of enzyme; for comparison, the very drastic (25-fold) reduction in the level of RNase E polypeptide that occurred upon arabinose withdrawal resulted in only 40% greater stabilization of pM1 compared to the effect of RraA. Furthermore, the data in Figure 4A indicate that the presence of an inhibitory concentration of RraA did not alter the size of the pM1 cleavage products suggesting that interaction of the protein with RNase E does not affect the cleavage site specificity of this enzyme. RraA also inhibited the processing of pM1 by the N-terminal catalytic domain of RNase E in strain KSL2009, although the effect was less dramatic than in cells expressing full-length RNase E.

Similar results were obtained in the processing of asn-tRNA (Figure 4B), which is also cleaved by RNase E (Ow and Kushner, 2002). In cells expressing RraA, 11% of asn-tRNA products corresponded to the full-length species of 210 and 230 nt. For comparison, the 210 and 230 nt species were undetectable when RraA was not expressed. These species accumulated to a maximum of 22% of the total asn-tRNA products in cells depleted of RNase E by arabinose withdrawal.

Genome-wide analysis of mRNA abundance at single gene resolution was carried out by two-color hybridization to DNA microarrays containing 4405 known and predicted *E. coli* ORFs (Blattner et al., 1997). In these experiments, the effect of RraA induction for 1.5 hr was compared with the consequences of RNase E depletion by arabinose withdrawal. RraA overexpression increased the relative abundance of more than 2000 *E. coli* transcripts, giving rise to an mRNA profile that was very similar, but not identical, to the transcript signature observed during RNase E depletion (Figure 5A). Notably, a number of transcripts involved in cell envelope biosynthesis and in anaerobic metabolism were affected. For some mRNAs, for example *amnI, msbB*, and *ptr* in the Figure 5A insert, RraA resulted in even greater stabilization than what was observed upon a 25-fold reduction in RNase E protein (the level obtained upon arabinose depletion as determined in Figure 2C). Previous experiments have shown that certain transcripts are destabi-

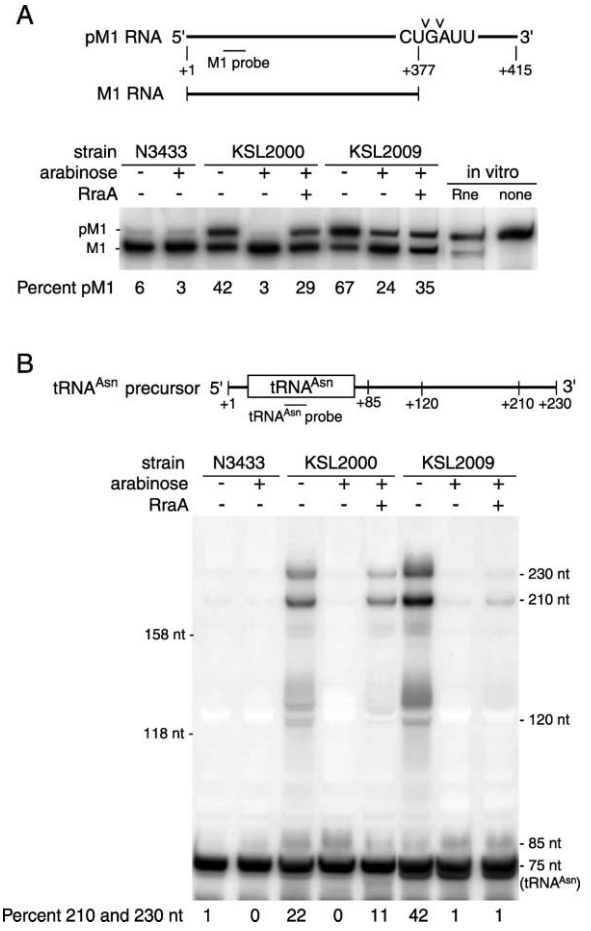

Figure 4. Effect of RraA on the Stability of RNase E Substrate RNAs

(A) Processing of pM1. Total RNA was isolated from KSL2000, KSL2009, and their parental strain N3433 overexpressing RraA (+) or no protein (−) from pTrc99A-derived plasmid and separated in a 6% PAGE containing 8 M urea. Separated RNA bands were transferred to a Nylon membrane and probed with ^{32}P end-labeled oligo complementary to M1 sequence. 10 ng of in vitro synthesized pM1 transcript (none) and its cleavage products by RNase E (Rne) were loaded in the last two lanes as size markers. Percentage pM1 RNA represents the ratio of pM1 to the sum of pM1 and M1 bands hybridized to the probe.

(B) Processing of RNA^{Asn}. Same procedure described in (A) was used except that the total RNA was separated by 8% PAGE containing 8 M urea and probed with an asn-tRNA specific probe. Percent 210 and 230 nt represents percentage ratio of the sum of the 210 and 230 nt bands to the sum of 75, 210, and 230 nt bands hybridized to the probe.

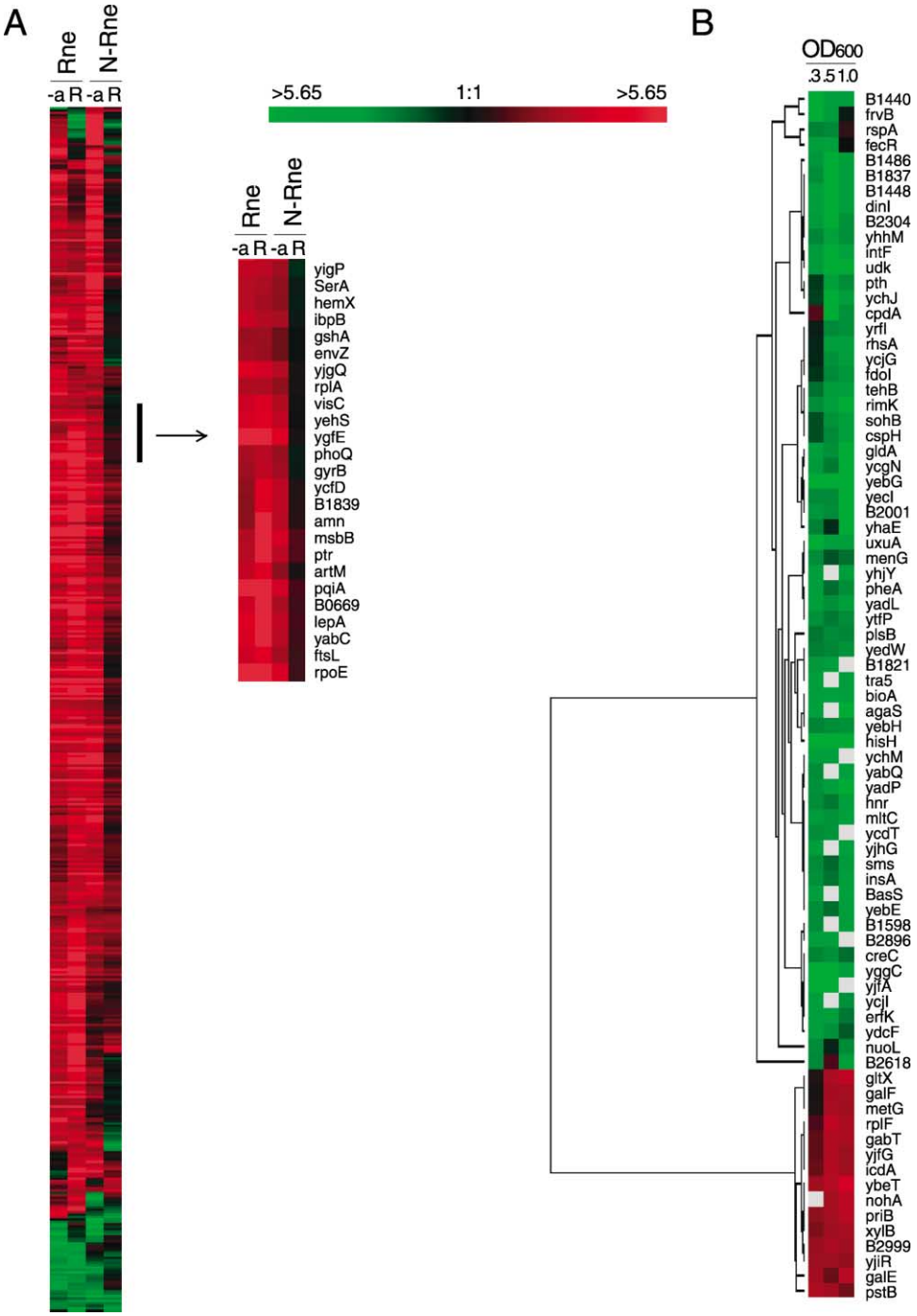

Figure 5. Effects of *rraA* Expression or Deletion on the Global Transcript Profile of *E. coli*

(A) Microarray analysis of RNA abundance. Genes whose relative mRNA levels were 2-fold or more changed in at least 2 out of 4 slides were clustered. Cy-5-labeled cDNAs were synthesized with RNA samples taken from strains: −a, KSL2000 plus pTrc99A (Rne) or KSL2009 plus pTrc99A (N-Rne) followed by withdrawal of arabinose for 1.5 hr; R, KSL2000 plus pTrc-RraA or KSL2009 plus pTrc-RraA. RNA samples from KSL2000 plus pTrc99A (Rne) or KSL2009 plus pTrc99A (N-Rne) grown in the presence of 0.1% arabinose were labeled with Cy-3 and comparisons between paired cultures were done directly.

(B) Hierarchical clustering of genes whose relative mRNA levels were 2-fold or more changed in at least 2 out of 3 slides. Cy-5-labeled cDNAs were synthesized with RNA samples taken from JCB570. RNA samples from JQ004 (*rraA*$^{-}$) were labeled with Cy-3 and comparisons between paired cultures were done directly. cDNA ratios are represented in tabular form according to the color scale shown at the top; rows correspond to individual genes and columns correspond to different strains (A) or growth phase (B). Red shades represent an increase in abundance and green shades represent a decrease in RNA abundance versus wild-type cells. Black indicates no detectable change in transcript level and gray represents the absence of data.

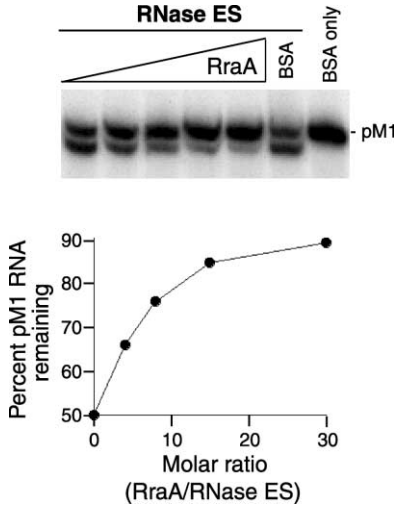

Figure 6. RraA Inhibits the *S. coelicolor* RNase E

Two picomoles of internally labeled pM1 RNA were incubated with 70 ng of RNase ES with varying concentrations of RraA or with 1 μg of BSA in 20 μl of 1× cleavage buffer at 37°C for 10 min.

lized by RNase E depletion (Lee et al., 2002), and these transcripts also showed decreased abundance during RraA expression.

We also analyzed the transcript profile in the complete absence of RraA. A null mutant, JQ004, lacking the entire chromosomal *rraA* coding sequence was constructed. This strain exhibited normal growth in minimal and rich media at 37°C. However, the absence of *rraA* altered the abundance of ~80 transcripts at least 2-fold (Figure 5B). Most of these RNAs were destabilized in JQ004, consistent with the inhibitory effect of RraA on the endoribonucleolytic activity of RNase E. Cells harvested in mid- or late-exponential phase or in early stationary phase exhibited generally similar transcript profiles.

E. coli RraA Also Inhibits the Endoribonucleolytic Activity of a *Streptomyces coelicolor* RNase E Ortholog In Vitro

Protein sequences homologous to RraA are distributed widely in Archae and proteobacteria and have also been identified in plants. Most of these organisms also contain one of three structural types of RNase E (Lee and Cohen, 2003). *Streptomyces coelicolor* contains a functional ortholog of *E. coli* RNase E and also an ORF showing 41% similarity to amino acid residues 29–118 of RraA. The recently characterized *S. coelicolor* functional ortholog (RNase ES) of *E. coli* RNase E was found to have similar cleavage site specificity to that of *E. coli* RNase E (Lee and Cohen, 2003). We evaluated the ability of RraA to inhibit the catalytic activity of RNase ES. As shown in Figure 6, RraA efficiently inhibited the cleavage action of RNase ES on pM1 RNA. 50% inhibition was observed at a 10:1 molar ratio of RraA monomer to RNase ES, which is identical to the degree of inhibition obtained with *E. coli* RNase E (Figures 3C and 3D).

Discussion

RraA represents a prototype for cellular proteins that modulate RNA decay and processing by binding to ribonucleases and inhibiting their activity. RraA did not interact detectably with RNA substrates or inhibit the binding of pM1 RNA to RNase E, suggesting that it affects the ability of RNase E to disrupt phosphodiester bonds between nucleotides by a mechanism that is independent of substrate binding. The absence of experimental evidence for binding of RraA to RNA substrates is supported by the crystal structure of RraA, which shows lack of any structural motif characteristic of nucleic acid binding (A.F. Monzingo et al., submitted). Earlier studies have shown that analogous RNA binding independent effects on hydrolysis can result from mutations in the *E. coli* endoribonuclease RNase III (Sun and Nicholson, 2001).

The RraA protein was isolated in a search for genes that, when expressed on a multicopy plasmid, enhance the yield of correctly folded human tissue plasminogen activator expressed in the *E. coli* periplasm. The higher tPA activity phenotype that we observed was the result of elevated expression of the disulfide isomerase DsbC protein, which in turn correlated with a dramatic increase in the steady-state abundance and half-life of the *dsbC* transcript. Inhibition of RNase E endoribonucleolytic activity by RraA in vitro and in vivo did not require the RNase E scaffold region, which contains sites for the binding of the major (PNPase, RhlB helicase, and enolase) and minor (GroEL, DnaK, and polyphosphate kinase) degradosome components indicating that these proteins do not play a primary role in the functional interactions we have observed between RraA and RNase E. However, RraA exhibited higher affinity and displayed more effective inhibition of RNA processing by the full-length RNase E relative to the catalytic domain. Our inability to detect binding of RraA to the N-terminal catalytic domain by coprecipitation or Far Western blotting or by in vitro assays using BIACORE analysis, suggests that despite the ability of RraA to inhibit the enzymatic activity of the N-terminal catalytic domain, the binding constant is probably greater than 200 μM. These observations suggest that the C-terminal scaffold region of RNase E enhances the ability of the catalytic domain of the ribonuclease to interact with RraA. Potentially, RraA may bind to multiple RNase E sites of which at least one is located in the N-terminal region and one or more is located in the CTH. Alternatively, deletion of the CTH may result in a conformational change in the N-terminal domain that reduces its affinity for RraA. The binding isotherm data are consistent with a single RraA binding site in RNase E and therefore support the second model. The notion that the CTH affects the conformation of the N-terminal domain is consistent with the differences in the substrate specificities of the two proteins. Interestingly, RNase G (Li et al., 1999), an RNase E paralog that is closely related to the N-terminal catalytic domain of RNase E (McDowall et al., 1993; Lee and Cohen, 2003) and which when overexpressed in *E. coli* confers viability on cells deleted for the RNase E-coding *rne* gene (Lee et al., 2002), is not inhibited by RraA.

Inhibition of RNase E by RraA is sufficiently strong to override the autoregulation of RNase E synthesis that normally maintains cellular RNase E activity within a narrow range, leading to prolongation of transcript half-life in vivo (for example, the *dsbC* transcript, Figure 1C).

Table 1. Strains and Plasmids Used in This Study

Strain/Plasmid	Description	Reference or Source
UT5600	F⁻ *ara-14 leuB6 azi-6 lacY1 proC14 tsx-67 Δ(ompT-fepC)266 entA403 trpE38 rfbD1 rpsL109 xyl-5 mtl-1 thi-1*	(Elish et al., 1988)
SF110	F⁻ *ΔlacX74 galE galK thi rpsL Δ phoA degP41 ΔompT*	(Baneyx and Georgiou, 1990)
JCB570	MC1000 *phoR zih12 : : Tn10*	(Bardwell et al., 1991)
JQ004	JCB570 *rraA*	This work
SY327	*araD Δ(lac-pro) argE(Am) recA56 rif^r nalA λpir*	(Miller and Mekalanos, 1988)
MC1061	*araD39 Δ(ara,leu)7697 ΔlacX74 galU⁻ galK⁻hsr⁻hsm⁺ strA*	(Casadaban and Cohen, 1980)
CJ1825	MC1061 *(λez1)*	(Jain et al., 2002)
CJ1825/BZ99	MC1061 *rne(1-602) (λez1)*	C. Jain
N3433	*lacZ43, relA, spoT, thi-1*	(Goldblum and Apirion, 1981)
KSL2000	*lacZ43, relA, spoT, thi-1 rne::cat, recA::Tn10* [pBAD-RNE]	(Lee et al., 2002)
KSL2009	Same as KSL2000 except [pBAD-NRNE]	This work
pBAD-stII-tPA	p15A *ori*, Cm^r, h-tPA with stII leader under PBAD	(Qiu et al., 1998)
pTrc-RraA	ColE1 ori, Amp^r, rraA under *trc* promoter	This work
pDW363	pBR *ori*, Amp^r, *birA*	(Tsao et al., 1996)
pDW363-RraA	pBR *ori*, Amp^r, *birA*, *rraA* under *trc* promoter	This work
pDW363-DsbA	pBR *ori*, Amp^r, *birA*, *dsbA* under *trc* promoter	This work
pBAD-RNE	pSC101 *ori*, Km^r, *rne* under PBAD	(Lee et al., 2002)
pBAD-NRNE	pSC101 *ori*, Km^r, *N-rne* under PBAD	This work
pRE107	*oriT*, *oriV*, Amp^r, *SacB*	(Edwards et al., 1998)
pET28A-RraA	f1 ori, Kan^r, rraA under T7 *lac* promoter	This work

In the absence of autoregulation, the effect of RraA on transcript accumulation is similar to that observed under severe RNase E depletion (Lee et al., 2002). Some of the physiological consequences that accompany the global changes in transcript abundance mediated by the overexpression of RraA include filamentation, the inability to grow at elevated temperatures (42°C), and a reduction in transcription from σ^{32} dependent promoters (J.Q., X.Z., and G.G., unpublished data; X.Z. and G.G., unpublished data). These effects are observed specifically in cells that express the full-length RNase E but not in strains that express the N-terminal catalytic domain, which is less sensitive to inhibition, suggesting that they result from RraA-mediated alteration of the transcript profile.

Extensive studies carried out during the last 20 years have established that proteins that bind to RNA substrates can competitively interfere with the decay and processing of these RNAs. Furthermore, both RNA decay and processing can be enhanced by the formation of ribonucleolytic "machines" (for reviews, see Cohen and McDowall, 1997; Coburn and Mackie, 1999; Steege, 2000). The discovery of RraA as an inhibitor of RNase E now establishes the existence of a fundamentally different, posttranslational level of control of RNA cleavages. It is noteworthy that the K_D value of 26 μM determined for the formation of a complex between RraA and full-length RNase E is of the same order as the equilibrium dissociation constant for proteins that perform regulatory functions such as, for example, transcription factors and core RNA polymerase enzyme (Scott et al., 2000).

What is the possible physiological significance of inhibition of RNA decay by RraA? As with other posttranslational mechanisms of regulation, RraA may facilitate rapid alterations in RNA decay and/or processing in response to specific environmental stimuli, although at this time, cellular conditions that may affect RraA production and/or activity have not been identified. In an *rraA* null strain cultured at 37°C with normal oxygenation in rich media, the number of transcripts affected was relatively small and the cells exhibited normal growth, suggesting that any physiological effects of RraA may occur under special growth conditions. The lack of a strong phenotype of an *rraA* null mutation also may be due to the presence of additional cellular proteins capable of modulating the catalytic function of RNase E and whose functions may partially overlap that of RraA. In fact, in separate genetic studies we found that *E. coli* expresses a second RNase E regulatory protein which we have designated RraB (J.G., K.L., M. Zhao, X.Z., J.Q., A. Saxena, S.N.C., G.G., unpublished data). Alternatively, the absence of *rraA* may lead to alterations in other features of ribonuclease regulation and a compensatory adjustment of the rate of RNA decay.

rraA-like genes are widely distributed in nature with homologs found in many organisms that contain endonuclease genes homologous to RNase E, including Archae, proteobacteria, and *Arabidopsis*. Moreover, our demonstration of functional crossreactivity of RraA on RNase E homologs from two distantly related bacterial species (i.e., *S. coelicolor* and *E. coli*) suggests that RraA may have a phylogenetically conserved function in modulating ribonuclease activity. While most organisms containing *rraA*-like genes also contain one of three structural types of RNase E (see Lee and Cohen, 2003), sequence analysis has not yet identified an RNase E homolog in six organisms that contain an *rraA* homolog. These include *Deinococcus radiodurans* and certain Archae. It is currently not known whether in these organisms RraA plays a role in RNA processing or has a different function.

Experimental Procedures

Strains and Plasmids

The strains and plasmids used in this work are listed in Table 1. The construction of the *rne* deleted *E. coli* strain KSL2000 has been previously described (Lee et al., 2002). KSL2009 was obtained by a plasmid displacement procedure. Briefly, introduction of an incompatible kanamycin resistance (Km^r) plasmid expressing N-RNase E

with a hexahistidine tag at the C terminus under the control of the BAD promoter (pBAD-NRNE) into KSL2004 (*rne*::*cat*, *recA*::*Tn10* [pRNG3]) (Lee et al., 2002), and selection for the incoming plasmid by growing transformants containing both plasmids (pBAD-NRNE and pRNG3) for 60 generations, resulted in displacement of the resident Amp^r plasmid by the Km^r N-Rne-expressing construct. pBAD-NRNE was constructed by replacing the NotI-SphI fragment, which contains the entire Rne-coding region of pBAD-RNE (Lee et al., 2002) with the NotI-SphI fragment from pNRNE4.

To construct the *rraA* null strain JQ004, the sequences flanking the 5′ and 3′ of the *rraA* gene were cloned into pRE107 (Edwards et al., 1998), the resulting plasmid was amplified in SY327 (Miller and Mekalanos, 1988) and transformed into the nonpermissive host strain JCB570 for allele exchange. Amp^R colonies were selected, and then transferred to sucrose-containing plates to counterselect for sucrose sensitivity.

Library Screening

E. coli UT5600 (*ompT*$^-$) genomic DNA was partially digested with Sau3AI and 2–4 kb DNA fragments were cloned into pTrc99A. The ligation mixture was transformed into SF110 (pBAD-stII-htPA) and colonies were patched onto LB plates, with and without 0.2% arabinose. Approximately 10,000 clones from a genomic library were grown on agar plates containing IPTG and arabinose (to induce the transcription of the insert DNA and h-tPA, respectively). After overnight incubation at 30°C, plates containing arabinose were treated with chloroform vapor for 30 min and overlaid with fibrin/agarose. Fibrin was formed by mixing fibrinogen and thrombin (Sigma, MO) (Qiu et al., 1998). Conversion of plasminogen to plasmin solubilizes the fibrin network resulting in the formation of a clearance zone representative of the tPA activity. Colonies expressing active tPA developed a zone of clearance over an opaque background.

Detection of Proteins In Vivo

For Western blot analysis, cells were grown in LB media and the synthesis of RraA was induced with 0.5 mM IPTG added at A_{600} ~0.2. After 1.5 hr, the cells were harvested, lysed by French press (2,000 psi) and equal amounts of protein were loaded onto SDS-PAGE gels. The protein band hybridizing to antibody was visualized using the SuperSignal Chemiluminescent Kit (Pierce, CA).

An in vivo biotinylated RraA protein was constructed by fusing a DNA sequence encoding a 21 amino acid peptide substrate for *E. coli* biotin holoenzyme synthetase (BirA) (Schatz, 1993) and cloned into vector pDW363 (Tsao et al., 1996), to generate plasmid pDW363-rraA that produces biotinylated RraA protein. Transformants were cultured in LB media containing 8 μg/ml of biotin (Sigma, MO) at 37°C and 1 mM of IPTG was added at A_{600} ~0.6. Three hours after induction, *E. coli* cells were harvested by centrifugation and resuspended in 1/5 volume of cold lysis buffer (150 mM sodium chloride, 1.0% NP-40, 50 mM Tris, [pH 8.0]). Following lysis by French press, aliquots containing 5 mg of lysate protein in 400 μl were mixed with 100 μl of streptavidin bead slurry (Amersham, Sweden) and incubated at 4°C for 1 hr. The streptavidin beads were recovered by centrifugation, washed 5 times with cold lysis buffer, resuspended in 100 μl of 2× SDS protein loading buffer, and RNase E was detected by Western blot.

Enzyme Assays

tPA activity was monitored using a fibrin plate assays as described (Qiu et al., 1998). β-galactosidase assays were performed in cells grown with or without 0.5 mM IPTG added at an A_{600} ~0.2 and harvested 1.5 hr after induction (Miller, 1992).

RNA Methods

RNA protection assays were performed in cells grown, induced, and harvested as above. An aliquot was harvested 1.5 hr after induction to determine the steady-state level of *dsbC* transcripts and the rest of the cells were treated with rifampicin at a final concentration of 200 μg/ml. Subsequently, cell samples harvested at different time points were rapidly chilled in an ethanol dry ice bath and total RNA was prepared using RNeasy kit (Qiagen). The amount of RNA was quantified spectrophotometrically at 260 nm and RNase protection assays were carried out using the RPA III kit (Ambion) with a probe-containing sequence complementary to the first 250 bp of *dsbC* gene.

To prepare total RNA from KSL2000 containing pTrc99A (no arabinose), cells were grown to mid-log phase in the presence of 0.1% arabinose, harvested, washed with LB medium two times, and reinoculated into LB medium containing no arabinose and grown at 37°C to an A_{600} ~0.2. 0.5 mM IPTG was added, the cells were harvested 1.5 hr later, and total RNA was prepared. Total RNA was isolated as described by Lin-Chao and Cohen (1991) and Northern blot analysis was performed as described previously (Lee et al., 2002). Oligonucleotide probes used were M1 (5′-GCTCTCTGTTGCACTGGTCG-3′) and tRNA^{Asn} (5′-TACGGATTAACAGTCCGCCGTTCTACCGACTGAA CTACAGA-3′) for pM1 RNA and tRNA^{Asn} processing, respectively.

Biochemical Methods

N-RNase E, RNase E, and RNase ES were purified from KSL2002, KSL2003, and *S. coelicolor* harboring pRNES301, respectively, as described previously (Lee et al., 2002; Lee and Cohen, 2003). RraA was purified from BL21(pET28A-RraA) by ion exchange chromatography on Mono Q HR 5/5 anion exchange column. The eluted proteins were concentrated by Centricon YM-3 Centrifugal Filter Devices (Millipore, MA).

Surface plasmon resonance was performed at 25°C using a BIACORE 3000® instrument (Biacore International AB, Sweden). 2500 RU each of Purified RNase E and bovine serum albumin were immobilized on different flow cells of a CM5 sensor chip using amine-coupling chemistry. Purified RraA at a concentration range of 0 to 100 μM was injected at a constant flow rate of 40 μl/min. Data were analyzed with BIAevaluation (version 3.2) software. The equilibrium dissociation constants (K_D) were calculated from the steady-state RU binding signal.

pM1 RNA transcript universally labeled with [α-^{32}P] UTP was synthesized as described previously (Lee et al., 2002) except that the purified pM1 RNA was denatured at 75°C for 10 min in 2 mM Tris-HCl [pH 7.6] and renatured by cooling down slowly to 30°C for 30 min in a heating block. RNase E cleavage assays were performed as described previously (McDowall et al., 1995) except that proteins (RNase E and RraA) and pM1 RNA were mixed in 1× cleavage buffer and preincubated on ice for 10 min before starting the cleavage reaction at 37°C.

Gel mobility shift assays were performed in 20 μl reactions with purified proteins (concentrations indicated in Figure 3B legend) and 50 ng of internally labeled pM1 RNA in the presence of 20 mM Tris-HCl [pH 7.6], 200 mM NaCl, 0.4 mM DTT, and 0.4 mM EDTA. The reaction mixtures were incubated for 10 min at room temperature, adjusted to 3% Ficoll (400), and loaded on 8% nondenaturing polyacrylamide gel with a crosslinking ratio of 19:1 in 100 mM Tris-HCl [pH 8.0], and 50 mM glycine buffer. Electrophoresis was carried out at 4°C at 240 V for 3 hr.

Gel filtration chromatography was performed on an AKTA FPLC with a Superdex 200 column (Amersham Biosciences). 0.5 ml gel filtration standards (Bio-Rad, CA) or purified RraA was applied to the column preequilibrated with 0.05 M Na_2HPO_4, 0.05 M NaH_2PO_4, 0.15 M NaCl, [pH 6.8] and eluted with the same buffer.

Microarray Procedures

Relative mRNA levels were determined by parallel two-color hybridization to DNA microarrays (Schena et al., 1995) on glass slides containing 4405 known and predicted ORFs. Comparative measurements of transcript abundance were performed by directly determining the abundance of each gene's transcripts relative to the wild-type sample, described by Khodursky et al. (2000).

Analysis of data was performed with the software available at http://genomewww4.stanford.edu/MicroArray/SMD/restech.html and http://rana.stanford.edu.

Acknowledgments

This work was supported by grants NSF BES-963406 and NIH GM 55090 to G.G., NIH GM 64511-01 to R.M., and by NIH GM 54158 to S.N.C. We thank J. Beckwith, A.J. Carpousis, J.G. Belasco, and S.R. Kushner for the gift of strains and S.R. Kushner and S. Lin-Chao for polyclonal antibodies to RNase E. We are grateful to C. Jain for

many useful suggestions, K. Ravi for running the HPLC analysis of quinone synthesis, A. Saxena for assistance with library screening, and A. Hayhurst for help with BIACORE analysis.

Received: May 20, 2003
Revised: July 16, 2003
Accepted: August 1, 2003
Published: September 4, 2003

References

Baneyx, F., and Georgiou, G. (1990). In vivo degradation of secreted fusion proteins by the Escherichia coli outer membrane protease OmpT. J. Bacteriol. *172*, 491–494.

Bardwell, J.C., McGovern, K., and Beckwith, J. (1991). Identification of a protein required for disulfide bond formation in vivo. Cell *67*, 581–589.

Bernstein, J.A., Khodursky, A.B., Lin, P.H., Lin-Chao, S., and Cohen, S.N. (2002). Global analysis of mRNA decay and abundance in *Escherichia coli* at single-gene resolution using two-color fluorescent DNA microarrays. Proc. Natl. Acad. Sci. USA *99*, 9697–9702.

Bessette, P.H., Qiu, J., Bardwell, J.C.A., Swartz, J.R., and Georgiou, G. (2001). The effect of the sequence of the active site dipeptide of DsbA and DsbC on the *in vivo* folding of multidisulfide proteins in *Escherichia coli*. J. Bacteriol. *183*, 980–988.

Blattner, F.R., Plunkett, G., 3rd, Bloch, C.A., Perna, N.T., Burland, V., Riley, M., Collado-Vides, J., Glasner, J.D., Rode, C.K., Mayhew, G.F., et al. (1997). The complete genome sequence of *Escherichia coli* K-12. Science *277*, 1453–1474.

Carpousis, A.J., Van Houwe, G., Ehretsmann, C., and Krisch, H.M. (1994). Copurification of *E. coli* RNAase E and PNPase: evidence for a specific association between two enzymes important in RNA processing and degradation. Cell *76*, 889–900.

Casadaban, M.J., and Cohen, S.N. (1980). Analysis of gene control signals by DNA fusion and cloning in *Escherichia coli*. J. Mol. Biol. *138*, 179–207.

Coburn, G.A., and Mackie, G.A. (1999). Degradation of mRNA in *Escherichia coli*: an old problem with some new twists. Prog. Nucleic Acid Res. Mol. Biol. *62*, 55–108.

Cohen, S.N., and McDowall, K.J. (1997). RNase E: still a wonderfully mysterious enzyme. Mol. Microbiol. *23*, 1099–1106.

Cormack, R.S., and Mackie, G.A. (1992). Structural requirements for the processing of *Escherichia coli* 5 S ribosomal RNA by RNase E *in vitro*. J. Mol. Biol. *228*, 1078–1090.

Edwards, R.A., Keller, L.H., and Schifferli, D.M. (1998). Improved allelic exchange vectors and their use to analyze 987P fimbria gene expression. Gene *207*, 149–157.

Elish, M.E., Pierce, J.R., and Earhart, C.F. (1988). Biochemical analysis of spontaneous fepA mutants of Escherichia coli. J. Gen. Microbiol. *134*, 1355–1364.

Feng, Y., Huang, H., Liao, J., and Cohen, S.N. (2001). *Escherichia coli* poly(A)-binding proteins that interact with components of degradosomes or impede RNA decay mediated by polynucleotide phosphorylase and RNase E. J. Biol. Chem. *276*, 31651–31656.

Feng, Y., Vickers, T.A., and Cohen, S.N. (2002). The catalytic domain of RNase E shows inherent 3' to 5' directionality in cleavage site selection. Proc. Natl. Acad. Sci. USA *99*, 14746–14751.

Georgellis, D., Barlow, T., Arvidson, S., and von Gabain, A. (1993). Retarded RNA turnover in *Escherichia coli*: a means of maintaining gene expression during anaerobiosis. Mol. Microbiol. *9*, 375–381.

Ghora, B.K., and Apirion, D. (1978). Structural analysis and in vitro processing to p5 rRNA of a 9S RNA molecule isolated from an rne mutant of *E. coli*. Cell *15*, 1055–1066.

Goldblum, K., and Apirion, D. (1981). Inactivation of the ribonucleic acid-processing enzyme ribonuclease E blocks cell division. J. Bacteriol. *43*, 128–132.

Gurevitz, M., Jain, S.K., and Apirion, D. (1983). Identification of a precursor molecular for the RNA moiety of the processing enzyme RNase P. Proc. Natl. Acad. Sci. USA *80*, 4450–4454.

Helmer-Citterich, M., Anceschi, M.M., Banner, D.W., and Cesareni, G. (1988). Control of ColE1 replication: low affinity specific binding of Rop (Rom) to RNAI and RNAII. EMBO J. *43*, 557–566.

Huang, H., Liao, J., and Cohen, S.N. (1998). Poly(A)- and poly(U)-specific RNA 3′ tail shortening by *E. coli* ribonuclease E. Nature *391*, 99–102.

Jain, C., and Belasco, J.G. (1995). RNase E autoregulates its synthesis by controlling the degradation rate of its own mRNA in *Escherichia coli*: Unusual sensitivity of the *rne* transcript to RNase E activity. Genes Dev. *9*, 84–96.

Jain, C., Deana, A., and Belasco, J.G. (2002). Consequences of RNase E scarcity in Escherichia coli. Mol. Microbiol. *43*, 1053–1064.

Kalapos, M.P., Paulus, H., and Sarkar, N. (1997). Identification of ribosomal protein S1 as a poly(A) binding protein in *Escherichia coli*. Biochimie *79*, 493–502.

Kadokura, H., Katzen, F., and Beckwith, J. (2003). Protein disulfide bond formation in prokaryotes. Annu. Rev. Biochem. *72*, 111–135.

Khodursky, A.B., Peter, B.J., Cozzarelli, N.R., Botstein, D., Brown, P.O., and Yanofsky, C. (2000). DNA microarray analysis of gene expression in response to physiological and genetic changes that affect tryptophan metabolism in *Escherichia coli*. Proc. Natl. Acad. Sci. USA *97*, 12170–12175.

Kido, M., Yamanaka, K., Mitani, T., Niki, H., Ogura, T., and Hiraga, S. (1996). RNase E polypeptides lacking a carboxyl-terminal half suppress a mukB mutation in Escherichia coli. J. Bacteriol. *178*, 3917–3925.

Lee, K., and Cohen, S.N. (2003). A *Streptomyces coelicolor* functional orthologue of *Escherichia coli* RNase E shows shuffling of catalytic and PNPase-binding domains. Mol. Microbiol. *48*, 349–360.

Lee, K., Bernstein, J.A., and Cohen, S.N. (2002). RNase G complementation of *rne* null mutation identifies functional interrelationships with RNase E in *Escherichia coli*. Mol. Microbiol. *43*, 1445–1456.

Leroy, A., Vanzo, N.F., Sousa, S., Dreyfus, M., and Carpousis, A.J. (2002). Function in *Escherichia coli* of the non-catalytic part of RNase E: role in the degradation of ribosome-free mRNA. Mol. Microbiol. *45*, 1231–1243.

Li, Z., and Deutscher, M.P. (2002). RNase E plays an essential role in the maturation of *Escherichia coli* tRNA precursors. RNA *8*, 97–109.

Li, Z., Pandit, S., and Deutscher, M.P. (1999). RNase G (CafA protein) and RNase E are both required for the 5′ maturation of 16S ribosomal RNA. EMBO J. *18*, 2878–2885.

Lin-Chao, S., and Cohen, S.N. (1991). The rate of processing and degradation of antisense RNAI regulates the replication of ColE1-type plasmids *in vivo*. Cell *65*, 1233–1242.

Lin-Chao, S., Wong, T.T., McDowall, K.J., and Cohen, S.N. (1994). Effects of nucleotide sequence on the specificity of rne-dependent and RNase E-mediated cleavages of RNA I encoded by the pBR322 plasmid. J. Biol. Chem. *269*, 10797–10803.

Lin-Chao, S., Wei, C.L., and Lin, Y.T. (1999). RNase E is required for the maturation of ssrA RNA and normal ssrA RNA peptide-tagging activity. Proc. Natl. Acad. Sci. USA *96*, 12406–12411.

Liou, G.G., Jane, W.N., Cohen, S.N., Lin, N.S., and Lin-Chao, S. (2001). RNA degradosomes exist in vivo in Escherichia coli as multicomponent complexes associated with the cytoplasmic membrane via the N-terminal region of ribonuclease E. Proc. Natl. Acad. Sci. USA *98*, 63–68.

Lopez, P.J., Marchand, I., Joyce, S.A., and Dreyfus, M. (1999). The C-terminal half of RNase E, which organizes the *Escherichia coli* degradosome, participates in mRNA degradation but not rRNA processing *in vivo*. Mol. Microbiol. *33*, 188–199.

Mackie, G.A. (1992). Secondary structure of the mRNA for ribosomal protein S20. Implications for cleavage by ribonuclease E. J. Biol. Chem. *267*, 1054–1061.

Mackie, G.A. (1998). Ribonuclease E is a 5′-end-dependent endonuclease. Nature *395*, 720–723.

McDowall, K.J., and Cohen, S.N. (1996). The N-terminal domain of the *rne* gene product has RNase E activity and is non-overlapping with arginine-rich RNA-binding site. J. Mol. Biol. *255*, 349–355.

McDowall, K.J., Hernandez, R.G., Lin-Chao, S., and Cohen, S.N.

(1993). The ams-1 and rne-3071 temperature-sensitive mutations in the *ams* gene are in close proximity to each other and cause substitutions within a domain that resembles a product of the *Escherichia coli mre* locus. J. Bacteriol. *175*, 4245–4249.

McDowall, K.J., Lin-Chao, S., and Cohen, S.N. (1994). A+U content rather than a particular nucleotide order determines the specificity of RNase E cleavage. J. Biol. Chem. *269*, 10790–10796.

McDowall, K.J., Kaberdin, V.R., Wu, S.-W., Cohen, S.N., and Lin-Chao, S. (1995). Site-specific RNase E cleavage of oligonucleotides and inhibition by stem-loops. Nature *374*, 287–290.

Meganathan, R. (1996). Biosynthesis of the isoprenoid quinones menaquinone (vitamin K_2) and ubiquinone (coenzyme Q). In *Escherichia coli* and *Salmonella*, F.C. Neidhardt, ed. (Washington, D.C.: ASM Press), pp. 642-656.

Miczak, A., Kaberdin, V.R., Wei, C.L., and Lin-Chao, S. (1996). Proteins associated with RNase E in a multicomponent ribonucleolytic complex. Proc. Natl. Acad. Sci. USA *93*, 3865–3869.

Miller, J.H. (1992). A Short Course of Bacterial Genetics (Cold Spring Harbor, N.Y.: Cold Spring Harbor Laboratory Press).

Miller, V.L., and Mekalanos, J.J. (1988). A novel suicide vector and its use in construction of insertion mutations: osmoregulation of outer membrane proteins and virulence determinants in Vibrio cholerae requires toxR. J. Bacteriol. *170*, 2575–2583.

Mudd, E.A., and Higgins, C.F. (1993). *Escherichia coli* endoribonuclease RNase E: autoregulation of expression and site-specific cleavage of mRNA. Mol. Microbiol. *9*, 557–568.

Ow, M.C., and Kushner, S.R. (2000). Analysis of mRNA decay and rRNA processing in *Escherichia coli* in the absence of RNase E-based degradosome assembly. Mol. Microbiol. *38*, 854–866.

Ow, M.C., and Kushner, S.R. (2002). Initiation of tRNA maturation by RNase E is essential for cell viability in *E. coli*. Genes Dev. *16*, 1102–1115.

Py, B., Higgins, C.F., Krisch, H.M., and Carpousis, A.J. (1996). A DEAD-box RNA helicase in the *Escherichia coli* RNA degradosome. Nature *381*, 169–172.

Qiu, J., Swartz, J.R., and Georgiou, G. (1998). Expression of active human tissue-type plasminogen activator in Escherichia coli. Appl. Environ. Microbiol. *64*, 4891–4896.

Raynal, L.C., and Carpousis, A.J. (1999). Poly(A) polymerase I of Escherichia coli: characterization of the catalytic domain, an RNA binding site and regions for the interaction with proteins involved in mRNA degradation. Mol. Microbiol. *32*, 765–775.

Schatz, P.J. (1993). Use of peptide libraries to map the substrate specificity of a peptide-modifying enzyme: a 13 residue consensus peptide specifies biotinylation in Escherichia coli. Biotechnology (N. Y.) *11*, 1138–1143.

Schena, M., Shalon, D., Davis, R.W., and Brown, P.O. (1995). Quantitative monitoring of gene expression patterns with a complementary DNA microarray. Science *270*, 467–470.

Scott, D.J., Ferguson, A.L., Gallegos, M.T., Pitt, M., Buck, M., and Hoggett, J.G. (2000). Interaction of sigma factor sigmaN with Escherichia coli RNA polymerase core enzyme. Biochem. J. *352*, 539–547.

Steege, D.A. (2000). Emerging features of mRNA decay in bacteria. RNA *6*, 1079–1090.

Sun, W., and Nicholson, A.W. (2001). Mechanism of action of *Escherichia coli* ribonuclease III. Stringent chemical requirement for the glutamic acid 117 side chain and Mn^{2+} rescue of the Glu117Asp mutant. Biochemistry *40*, 5102–5110.

Taraseviciene, L., Bjork, G.R., and Uhlin, B.E. (1995). Evidence for an RNA binding region in the *Escherichia coli* processing endoribonuclease RNase E. J. Biol. Chem. *270*, 26391–26398.

Tsao, K.L., DeBarbieri, B., Michel, H., and Waugh, D.S. (1996). A versatile plasmid expression vector for the production of biotinylated proteins by site-specific, enzymatic modification in Escherichia coli. Gene *169*, 59–64.

Vanzo, N.F., Li, Y.S., Py, B., Blum, E., Higgins, C.F., Raynal, L.C., Krisch, H.M., and Carpousis, A.J. (1998). Ribonuclease E organizes the protein interactions in the *Escherichia coli* RNA degradosome. Genes Dev. *12*, 2770–2781.

Walsh, A.P., Tock, M.R., Mallen, M.H., Kaberdin, V.R., von Gabain, A., and McDowall, K.J. (2001). Cleavage of poly(A) tails on the 3′-end of RNA by ribonuclease E of *Escherichia coli*. Nucleic Acids Res. *29*, 1864–1871.

Zhan, X. (2002). Genetic studies of disulfide bond isomerization in *E. coli*. PhD thesis. The University of Texas at Austin, Austin, Texas.